

# The Molecular Basis of Fracture in Crosslinked Glassy Polymers

M. SAMBASIVAM,<sup>1-3,6,\*</sup> A. KLEIN,<sup>1,2,4,5</sup> L. H. SPERLING<sup>1-4</sup>

<sup>1</sup> Polymer Interfaces Center, Lehigh University, Bethlehem, Pennsylvania 18015-3194

<sup>2</sup> Center for Polymer Science and Engineering, Lehigh University, Bethlehem, Pennsylvania 18015-3194

<sup>3</sup> Materials Research Center, Lehigh University, Bethlehem, Pennsylvania 18015-3194

<sup>4</sup> Department of Chemical Engineering, Lehigh University, Bethlehem, Pennsylvania 18015-3194

<sup>5</sup> Emulsion Polymers Institute, Lehigh University, Bethlehem, Pennsylvania 18015-3194

<sup>6</sup> Department of Chemistry, Lehigh University, Bethlehem, Pennsylvania 18015-3194

Received 6 May 1996; accepted 1 January 1997

**ABSTRACT:** Crosslinked polystyrene (XPS) and poly(methyl methacrylate) (XPMMA) were prepared by photopolymerization of the respective monomers in the presence of reversible crosslinkers, acrylic acid anhydride (AAA), and methacrylic acid anhydride (MAA). Fracture studies on the crosslinked samples were carried out using a Dental Burr Grinding Instrument (DBGI). The fracture energy in all cases showed a maximum around 1.5–5.0 mol % crosslinker. The samples were decrosslinked by hydrolysis using dilute aqueous ammonium hydroxide solutions to determine the number of chain scissions as a result of grinding. The number of chain scissions increased asymptotically with crosslink density in the range of a 0.0–10.0 mol % crosslinker. The number of bonds activated per scission, obtained from the calculated total chain scission energy (after subtracting the chain pullout energy) and the experimental number of chain scissions, remained fairly constant for AAA-PS and AAA-PMMA at  $312 \pm 150$  bonds and  $202 \pm 50$  bonds, respectively, in the region below the fracture energy maximum. In an attempt to explain the fracture energy increases, increasing physical entanglements with crosslinking is considered. © 1997 John Wiley & Sons, Inc. *J Appl Polym Sci* **65**: 1001–1011, 1997

## INTRODUCTION

Crack propagation in polymers is accompanied by various molecular processes, namely chain uncoiling, scission, and pullout, as two new surfaces are

created. For glassy, linear, amorphous polymers, the last two mechanisms are the most important,<sup>1,2</sup> with their relative contribution dependent on molecular weight, temperature, etc. There is extensive literature on the fracture behavior of polymers addressing both the molecular<sup>3</sup> and fracture mechanics approaches.<sup>4</sup>

In crosslinked polymers, however, one would expect a higher contribution from chain scission due to the presence of permanent chemical crosslinks, limiting the mobility. In an ideal case of an end-crosslinked, perfect network, chain scission should be the only possible molecular mechanism

\* Present address: Polyset Company, P. O. Box 111, Mechanicville, NY 12118.

Correspondence to: L. H. Sperling.

Contract grant sponsor: National Science Foundation; contract grant number: ECD-9117064.

Contract grant sponsor: National Science Foundation; contract grant number: MSS-9212805.

© 1997 John Wiley & Sons, Inc. CCC 0021-8995/97/051001-11

of failure. For lightly crosslinked real networks, there might still be a considerable contribution from chain pullout during fracture due to the presence of chain imperfections such as dangling chain ends and loops. Physical entanglements also contribute to the mechanical properties of networks,<sup>5</sup> providing quasi-permanent bonds in the glassy state.

Crosslinking is of significant industrial importance to reduce creep, and improve solvent resistance. While fracture studies on crosslinked plastics were limited mainly to the fracture energy,  $G_{IC}$ ,<sup>6,7</sup> and tensile measurements,<sup>8</sup> Natarajan and Reed<sup>9</sup> considered the molecular aspects of fracture in elastomers. They observed chain scission in natural rubber during tensile testing at low temperatures (150 K) below the glass transition temperature ( $T_g$ ), using electron spin resonance spectroscopy (ESR). The number of free radicals detected by ESR increased with crosslink density.

In polymer networks, the role of physical entanglements is still an issue of great controversy. Recently, Gent et al.<sup>10</sup> studied the contribution from physical entanglements to the modulus of endlinked poly(dimethyl siloxane) networks and homo-interpenetrating networks (homo-IPNs). While the modulus of the networks, end-crosslinked and still in the dilute state, followed simple rubber elasticity theory, the modulus of highly end-crosslinked, undiluted networks was anomalously high. This was attributed to the contribution from extra physical entanglements. On the other hand, studies of homo-IPNs of polystyrene<sup>11-14</sup> revealed no added physical entanglements.

Previous studies from Lehigh University focussed on the latex film formation processes in linear polystyrene (PS) of different molecular weights<sup>1,2,15</sup> and PMMA.<sup>16</sup> Using a custom-built Dental Burr Grinding Instrument (DBGI), which grinds at an average depth of 500 nm per pass (several times the diameter of the latex particles), the fracture energy was determined. From the molecular weight reduction, the number of chain scissions were obtained, which was then used to calculate the scission and uncoiling energies. The remaining energy was ascribed to chain pullout. Correlation between the molecular weight, chain scission, and chain pullout contributions to the total fracture energy was observed in PS latex films. At the low molecular weight end, about 32,000 g/mol, which is the critical limit for

entanglements ( $\sim 2 M_e$ , where  $M_e$  is the molecular weight between entanglement points) for PS, the fracture energy is mainly due to chain pullout (near 100%).<sup>2</sup> With increasing molecular weights, the contribution from chain pullout energy decreased to about 50% at 151,000 g/mol<sup>2</sup> and, to about 10% at 420,000 g/mol.<sup>1</sup> Similar results were obtained for PMMA<sup>16</sup>; the somewhat lower values of  $M_e$  for PMMA resulted in higher fracture energies.

The objective of this work is to investigate the influence of crosslinking on the extent of chain scission and pullout processes and the fracture energy in crosslinked polystyrene (XPS) and crosslinked PMMA (XPMMA). Molecular weight measurements to determine the number of scissions due to grinding fracture were possible by using reversible crosslinkers, acrylic acid anhydride (AAA), and methacrylic acid anhydride (MAA), which can be decrosslinked by hydrolysis in warm ammonium hydroxide solution.<sup>17</sup>

## EXPERIMENTAL

### Synthesis of XPS and XPMMA

Styrene and methyl methacrylate monomers were purified by passing through an alumina column. Other materials were used as received. The XPS and XPMMA polymers were prepared by photopolymerization of styrene and methyl methacrylate monomers, respectively, induced by ultraviolet (UV) light in the presence of crosslinkers, AAA, and MAA. Benzoin was used as the initiator (0.5 wt %). A mixture of the monomer, initiator, and crosslinker were poured into a glass mold with spacer ring, after degassing with nitrogen for 1 min. The mol % of the crosslinker was varied from 0 to 20 mol %. After photopolymerization for 48 h, the samples were dried in a vacuum oven at 130°C for 48 h to remove the residual monomer. Drying was verified by the increase in glass transition temperatures to about 108°C for XPS and about 125°C for XPMMA via differential scanning calorimetry (DSC) at a heating rate of 10°C/min. Also, the  $T_g$  increased with increasing crosslinker.

### Gel Fraction Studies

The amount of gel fraction in the crosslinked materials were determined gravimetrically. A known

weight (about 20 mg) of each crosslinked sample was allowed to swell in about 30 mL of swellant, at about 50°C for 7 days in a closed glass vial with occasional gentle agitation. Solvent was renewed, to ensure complete removal of the soluble portion, after 3 days. After solvent removal, the remaining sample was dried in a vacuum oven at about 100°C to constant weight.

### Crosslink Density Measurements

The crosslink density of the networks were measured by two different methods:

#### Equilibrium Swelling

The crosslink density was measured gravimetrically by swelling the samples in 500 times the volume of solvent, allowing 24 h for equilibrium and by using the Flory–Rehner<sup>18</sup> equation:

$$-\{[\ln(1 - v_2) + v_2 + \chi v_2^2]\} \\ = n V_1 [v_2^{1/3} - v_2/2] \quad (1)$$

where,  $v_2$  is the volume fraction of the polymer in the swollen state,  $\chi$  is the interaction parameter,  $n$  is the crosslink density (mol/cm<sup>3</sup>) and  $V_1$  is the molar volume of the solvent. Toluene and chloroform were used as swellants for XPS and XPMMA, respectively. Because eq. (1) holds only for low crosslink densities, the crosslink densities for films with higher mol % (>5 mol %) crosslinker were determined only from stoichiometry. The molecular weight between crosslinks,  $M_C$ , is given by

$$M_C = \rho/n \quad (2)$$

where  $\rho$  is the density of the polymer, and  $n$  is the crosslink density.

#### Rubbery Plateau Modulus

These experiments were carried out in a Rheometrics RDA dynamic mechanical analyzer. At a torsional frequency of 1 Hz, the shear modulus was measured at 165°C, which is in the rubbery plateau region. Based on rubber elasticity theory, the crosslink density or the active network chain segment density,  $n$ , is given by<sup>19</sup>:

$$n = G'/gRT \quad (3)$$

where  $G'$  is shear storage modulus,  $g$  is  $(f-2)/f$ , and  $f$  is the functionality of the crosslinker ( $f = 4$  for AAA and MAA),  $R$  is gas constant, and  $T$  is the plateau temperature (about 165°C). This equation is also limited to crosslink densities up to about 5 mol %.

### Fracture Experiments

Fracture of all the films was carried out on the DBGI at room temperature, with water cooling of the dental burr (FG 7572 carbide burr; SS White Co.). A constant burr rotational frequency of 16 Hz was used. The instrument measures the torque at the burr, which is plotted as a function of time. From the area under the torque curves, the fracture energy is obtained. To determine the number of chain scissions as a result of the grinding, the samples (a portion of the initial sample and the ground powder) were decrosslinked using dilute ammonium hydroxide solution (0.1  $N$ ) at 40°C for 48 h, prior to molecular weight measurements. For higher crosslink densities, prolonged hydrolysis (about 7 days) was required before molecular weight analysis.

### Ground Particle Surface Area

The surface area of the ground powder was determined using photon correlation spectroscopy (Coulter N4MD Analyzer), which yields the average diameter of the particles. The ground powder in water was homogenized using a sonifier (Ultrasonic Model W350). This was carried out in a plastic beaker for 90 s, before the spectroscopic analysis.

### Calculations

Two independent measurements were made during the experiments: the total energy to fracture a unit volume (or unit area) of polymer, and the molecular weight reduction. This permits the results to be expressed as two independent numbers: the number of chain scissions, and the number of chain pullouts, both expressed as either per unit volume or per unit area.

The total fracture energy per unit volume,  $E_T$ , obtained from the area under the torque curves (from DBGI) and the volume of the ground material, is divided into three different portions:

$$E_T = E_U + E_S + E_P \quad (4)$$

where  $E_U$ ,  $E_S$ , and  $E_P$  are the energies for uncoiling, scission, and pullout processes, respectively. In this work, the chain pullout energies were calculated theoretically using Evans approach.<sup>20</sup> The average molecular weight of the chain ends beyond the last crosslink (chemical) was used in the calculation. The remaining energy was ascribed to chain scission process. The change was made so as to permit the evaluation of the role of chemical vs. physical crosslinks more effectively. This is the reverse of previous studies.<sup>1,2,15,16</sup>

Because the uncoiling energy,  $E_U$ , is less than 1% of the total fracture energy,<sup>1,2</sup> its contribution was ignored. It could be argued that chain uncoiling in the glassy state probably consumes a considerable portion of the total fracture energy. However, it is possible that the scission energy in the present work contains some contributions from the uncoiling process, which is not discernible at this point.

The number of chain scissions per unit volume,  $N_v$ , is obtained from the initial and final number-average molecular weight,  $M_n^\circ$  and  $M_n$ , corresponding to before and after fracture, respectively:

$$N_v = A \cdot \rho \cdot (1/M_n - 1/M_n^\circ) \quad (5)$$

where  $\rho$  is the density of the polymer, and  $A$  is the Avogadro's number. The initial number-average molecular weights for the uncrosslinked PS and PMMA (0 mol % crosslinker), prepared by photopolymerization were 70,000 g/mol (PDI = 3.8) and 60,000 g/mol (PDI = 3.5), respectively. For the crosslinked samples, the initial molecular weight of each system was determined before fracture by the decrosslinking step followed by GPC analysis. A similar procedure was carried out on the ground portion after fracture to obtain the

**Table I Gel Fraction in XPS and XPMMA**

mol % Crosslinker	PS-AAA	PS-MAA	PMMA-AAA
0.0	0.0	0.0	0.0
0.5	34.0	58.0	89.0
1.0	61.0	NA	97.0
1.5	61.0	75.0	98.0
5.0	89.0	97.0	99.0
10.0	93.0	99.5	99.5

NA—not available.

**Table II Swelling Measurements on XPS**

mol % Crosslinker	$M_{Cswell}$ g/mol		$M_{Cstoich.}$ g/mol	
	AAA	MAA	AAA	MAA
0.0	$\infty$	$\infty$	$\infty$	$\infty$
0.5	132,000	127,000	12,600	15,400
1.0	74,200	NA	6,300	7,700
1.5	30,600	10,300	4,200	5,100
5.0	2,530	1,300	1,300	1,540
10.0	NA	NA	650	770
20.0	NA	NA	325	385

NA—not available.

AAA—acrylic acid anhydride.

MAA—methacrylic acid anhydride.

final molecular weight. The number of chain scissions per unit area,  $N_a$ , is given by:

$$N_a = (D_{avg}/6) \cdot N_v \quad (6)$$

where  $D_{avg}$  is the average diameter of the ground particles.

## RESULTS

### Gel Fraction Studies

Table I lists the gel fraction determined for the different networks. The AAA crosslinked PS has a lower amount of gel fraction, suggesting poor crosslinking of the chains, while the MAA crosslinked PS and AAA crosslinked PMMA have higher gel fraction.

### Swelling Measurements of PS and PMMA Networks

Tables II and III show the results of the swelling experiments for XPS and XPMMA, respectively.

**Table III Swelling Measurements on XPMMA Containing AAA**

mol % Crosslinker	$M_{Cswell}$ g/mol	$M_{Cstoich.}$ g/mol
0.0	$\infty$	$\infty$
0.5	11,500	12,600
1.0	5,200	6,300
1.5	2,400	4,200
5.0	1,100	1,300
10.0	NA	650
20.0	NA	325

AAA—acrylic acid anhydride.

NA—not available.

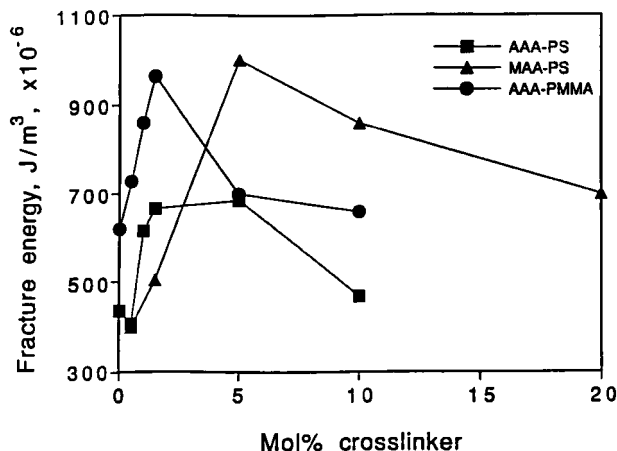


**Figure 1** Plot of fracture energy vs. mol % crosslinker for XPS and XPMMA (AAA—acrylic acid anhydride; MAA—methacrylic acid anhydride).

The initial weight of the polymer used in the calculations was corrected for the gel fraction given by Table I. For XPS, the crosslinking is poor up to about 1.5 mol % crosslinker for both AAA and MAA crosslinkers. Also, the crosslink densities of the MAA crosslinked samples are higher than that of the corresponding AAA crosslinked samples. The AAA monomer is known to cyclize to some extent. This formed the basis for preferring MAA as crosslinker.

In the case of XPMMA (Table III), the crosslink densities of AAA crosslinked networks are comparable to the stoichiometric values. Due to poor copolymerization reactivity ratios, the MAA crosslinked PMMA materials were not considered.

### Fracture Experiments

Figure 1 shows the plot of fracture energy vs. mol % crosslinker for XPS and XPMMA. It is evident that crosslinking increases the fracture energy significantly. A maximum in the fracture energy is observed at about 5 mol % crosslinker for both AAA and MAA crosslinked PS and at about 1.5 mol % for AAA crosslinked PMMA. At higher crosslink densities, MAA crosslinked PS retain their mechanical strength compared to the uncrosslinked sample (0 mol %) and the AAA crosslinked PS.

The above fracture behavior is not expected based on the Lake and Thomas theory,<sup>21</sup> according to which the fracture energy decreases with decreasing  $M_C$  ( $G_{IC} \sim M_C^{1/2}$ ), where  $M_C$  is the molecular weight between crosslinks. An im-

portant question is: why does a maximum in the fracture energy occur?

Flory et al.<sup>8</sup> observed a similar maximum in the tensile strength of natural rubber at about 10 mol % crosslinker. Recently, Sundell et al.<sup>22</sup> studied the effect of crosslinker mol % and its structure on the stress to break in crosslinked PS. Various divinyl crosslinkers were used. A maximum in the stress to break was observed in all cases. They also found that by increasing the flexibility of the crosslinker (by increasing the number of  $-\text{CH}_2-$  groups in the crosslinker), the stress to break increased.

However, Pearson and Yee's<sup>23</sup> results for epoxy systems showed no maximum. The stress intensity factor,  $K_{IC}$ , which is a measure of the fracture toughness in these systems decreased with increasing crosslinking. Also, for rubber toughened epoxies, this decrease in the  $K_{IC}$  was very significant. Probably these crosslinking levels were beyond the maximum.

Figure 2 shows the number of chain scissions per unit volume of ground material vs. the inverse of molecular weight between chemical crosslinks,  $M_C$  (obtained from swelling). The number of scissions increases asymptotically with crosslinking, the number of scissions being higher than the value for the uncrosslinked polymer (0.0 mol %) in all cases. Interestingly, no maximum is observed in the number of chain scissions per unit volume, unlike the fracture energy plot (see Fig. 1). This difference could be attributed to the chain pullout contribution.

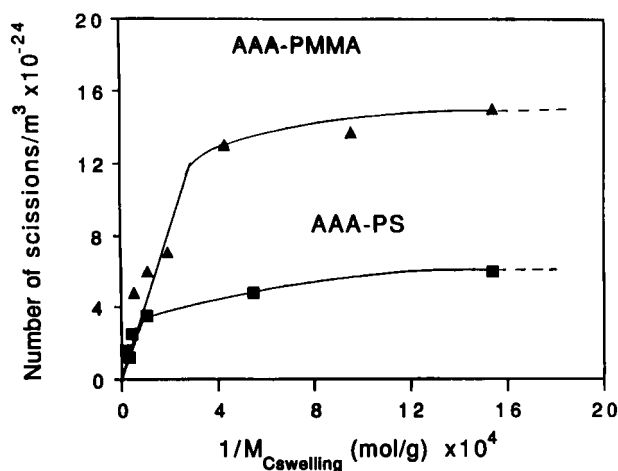


**Figure 2** Plot of the number of chain scissions vs. the inverse of molecular weight between chemical crosslinks in XPS and XPMMA (AAA—acrylic acid anhydride).

**Table IV Results of Surface Area Measurements in XPS and XPMMA**

mol % Crosslinker	Surface Area (m <sup>2</sup> /g)	Fracture Energy	
		$G_{BG}$ (J/m <sup>2</sup> )	$E_T^a$ (J/m <sup>3</sup> ) $\times 10^{-6}$
PS-MAA			
0.0 <sup>b</sup>	NA	NA	450
0.0 <sup>c</sup>	2.0	230	459
0.5	7.4	54	400
5.0	5.0	200	1000
10.0	5.5	156	860
PMMA-AAA			
0.0 <sup>d</sup>	NA	NA	620
0.5	7.5	97	728
1.5	6.0	161	964
10.0	5.8	123	713

<sup>a</sup> Error:  $\pm 15\%$ .

<sup>b</sup> Initial  $M_n = 70,000$  g/mol ( $M_w/M_n = 3.8$ ) (photopolymerized).

<sup>c</sup> Initial  $M_n = 151,000$  g/mol ( $M_w/M_n = 1.02$ ); fully annealed latex films, see ref. 2 in text.

<sup>d</sup> Initial  $M_n = 60,000$  g/mol ( $M_w/M_n = 3.5$ ).

PS-MAA—methacrylic acid anhydride crosslinked PS.

PMMA-AAA—acrylic acid anhydride crosslinked PMMA.

### Fracture Surface Area vs. Volume

The present work has reported the results of the fracture experiments in terms of per unit volume instead of the conventional per unit area basis. This is mainly because the fracture surface generated is highly irregular, and the use of euclidean geometry to describe a fractal surface might lead to substantial error. However, by measuring the average size of the ground powder (from the grinding experiments) using photon correlation spectroscopy, the surface area generated due to fracture was estimated. Via this route, it is possible to express the fracture energy in terms of per unit area. Equation (7) gives the simple relationship between the fracture energy per unit volume ( $E_T$ ) and the fracture energy per unit area ( $G_{BG}$ , where BG represents Burr Grinding):

$$G_{BG} = (D_{avg}/6) \cdot E_T \quad (7)$$

where  $D_{avg}$  is the number-average size of the ground particles.

Table IV lists the surface area generated and the fracture energy in terms of per unit area and per unit volume for selected samples. The fracture surface area generated per gram of ground material is decreasing slightly with increasing mol % crosslinker. It is to be pointed out that the  $G_{BG}$  value of 230 J/m<sup>2</sup> for uncrosslinked PS is on the lower side of the reported values of  $G_{IC}$  for PS

(200–1000 J/m<sup>2</sup>). The variation in the  $G_{IC}$  values for PS in literature was attributed to the differences in the sharpness of the crack.<sup>24a</sup>

## DISCUSSION

### Energy Contributions

From the total fracture energy and the number of chain scissions, the energy contributions in the networks were determined. As mentioned earlier, a slightly different approach than that for the linear polymers was taken. For the linear systems,<sup>1,2,15,16</sup> the contributions due to chain uncoiling and chain scission were calculated from the number of chain scissions and the total fracture energy. About 300 bonds for PS and about 190 bonds for PMMA between entanglement points<sup>24b</sup> were considered to be activated before one bond broke, based on Lake and Thomas's theory.<sup>21</sup> The remainder portion of the total fracture energy was assumed to be due to chain pullout process. In the case of crosslinked samples, due to the presence of chemical and physical crosslinks, this model cannot be applied and, hence, a different approach was required.

Chain pullout energy contributions in the networks was determined using two different theoretical approaches: the Evans model<sup>20</sup> and the Mark approach.<sup>25</sup> According to Evan's model, un-

**Table V Energy Contributions in XPS (Based on Theoretical Pullout Energy)**

mol % AAA	$n$ , mol/cm <sup>3</sup> (Swelling)	Evans Theory		Mark Theory		Bonds Activated per Scission	
		% $E_P$	% $E_S$	% $E_P$	% $E_S$	Evans	Mark
0.0	NA	47.0	54.0	76.0	24.0	400	134
0.5	$2.0 \times 10^{-5}$	30.0	70.0	60.0	40.0	365	222
1.0	$4.6 \times 10^{-5}$	12.0	88.0	31.0	69.0	442	288
1.5	$1.1 \times 10^{-4}$	5.0	95.0	18.0	82.0	365	293
5.0	$5.8 \times 10^{-4}$	0.5	99.5	5.0	95.0	310	316
10.0	NA	0.2	99.8	4.0	96.0	160	204

NA—not available.

%  $E_S$  and %  $E_P$  are chain scission and pullout energies' contributions, respectively.

der chain pullout conditions, the chain pullout energy is given by,

$$E_P = kTN_e^2 \quad (8)$$

where  $E_P$  is the chain pullout energy per chain,  $k$  is Boltzmann constant,  $T$  is temperature (298 K), and  $N_e$  is the number of mers between the entanglement points for a linear material. For crosslinked systems, chain pullout is limited to chain ends. Hence,  $N_e$  is the number of mers in the chain ends, which is obtained from the swelling crosslink density, assuming a uniform crosslinking. The total chain pullout energy is obtained by multiplying eq. (8) by the number of chain end segments per unit volume. This latter is calculated from the number of chains present before fracture (determined by decrosslinking), which yields the total number of chain ends.

According to the Mark approach<sup>25</sup>, a —C—C— bond is considered broken when stretched by a distance equal to 1 Å from its equilibrium distance of 1.54 Å, and the energy associated with this process being 80 kcal/mol. Assuming that one-half of this energy is required to pull out a chain end segment on average, the pullout energy was calculated. The number of chain end segments was obtained from the decrosslinking procedure, as mentioned before.

From the difference between the total fracture energy and the calculated chain pullout energy,  $E_P$ , the chain scission energy,  $E_S$ , was obtained. Again, the minor contribution from the chain uncoiling process is ignored.

Results of these calculations are shown in Tables V and VI for AAA crosslinked PS and PMMA, respectively. Both approaches yield similar re-

sults, though the pullout contribution from Mark approach is higher. (In the case of linear PS and PMMA,<sup>2,15,16</sup> the chain pullout energy obtained from the Mark approach was higher by a factor of 2 compared to the Evans model, with the experimental values between these two values.) As expected, the scission energy contribution dominates at all crosslink levels, except in the case of 0.0 and 0.5 mol % XPS. It increases to about 95–99% around 5.0 mol % crosslinker in both XPS and XPMMA. Chain pullout energy contribution is significant at low crosslink levels. At high crosslinking level, however, this contribution becomes less important. This is also supported by the amount of gel fraction (Table I) present in the networks. With increasing gel fraction, the chain pullout contribution decreases. Also, the pullout contributions arises from the gel fraction due to defects such as chain ends, some containing the initiator fragment, which also get shorter.

An interesting outcome of these calculations is the estimation of the number of bonds activated per scission. This was extracted from the calculated chain scission energy,  $E_S$ , the number of chain scissions per unit volume,  $N_v$ , and the bond energy (about 80 kcal/mol). Tables V and VI list the values obtained for AAA crosslinked PS and PMMA, respectively, from the two theoretical approaches. The values from both theories are roughly constant, independent of the crosslink density, up to 5.0 mol % crosslinker for PS and up to about 1.5 mol % crosslinker for PMMA. It should be noted that the fracture energy and the number of scissions increased at nearly the same rate in this range, which explains the constancy in the number of activated bonds per scission. In the case of PS, an average value of 376 bonds

**Table VI Energy Contributions in XPMMA (Based on Theoretical Pullout Energy)**

mol % AAA	$n$ , mol/cm <sup>3</sup> (Swelling)	Evans Theory		Mark Theory		Bonds Activated per Scission	
		% $E_P$	% $E_S$	% $E_P$	% $E_S$	Evans	Mark
0.0	NA	17.0	83.0	32.0	68.0	220	179
0.5	$1.3 \times 10^{-4}$	3.0	97.0	13.0	87.0	240	215
1.0	$2.3 \times 10^{-4}$	1.0	99.0	8.0	92.0	244	231
1.5	$5.2 \times 10^{-4}$	1.0	99.0	4.0	96.0	140	147
5.0	NA	0.3	99.7	4.8	95.2	103	99
10.0	NA	0.2	99.8	3.2	96.8	90	87

NA—not available.

%  $E_S$  and %  $E_P$  are chain scission and pullout energies' contributions, respectively.

(Evans) and 251 bonds (Mark), and for PMMA, an average value of 211 bonds (Evans) and 193 bonds (Mark) are obtained. Considering the simplicity of the two theories, the agreement is very good and support the constancy in the number of activated bonds.

For linear PS and PMMA, the number of activated bonds is assumed to be the length between physical entanglements,<sup>1,2</sup> which is about 300 bonds and 190 bonds,<sup>24</sup> respectively. In other words, these values indicate that the segment length activated in the network is constant and corresponds approximately to the length between physical entanglements, independent of the chemical crosslink density, up to a certain crosslinker level (about 1.5–5.0 mol % in both cases). Again, the increasing total number of scissions is where the extra energy consumption is apparently going. At high crosslink levels ( $M_C \ll M_e$ , where  $M_C$  and  $M_e$  are the molecular weight between chemical crosslinks and physical entanglement points, respectively), the chemical crosslinks dominate. Hence, beyond 5 mol % crosslinker the number of bonds activated decreases, but the values are slightly higher than the actual number of bonds between the chemical crosslinks. The fracture energy apparently decreases in this region due to fewer bonds being activated per scission with decreasing  $M_C$ , in agreement with the Lake and Thomas theory.<sup>21</sup>

It must be noted that the temperature of the actual fracture surface, and chains being pulled out or scissioned, was estimated to be between 150–350°C for both PS and PMMA, well above  $T_g$ .<sup>2,15,16,26,27</sup> Thus, the chains are believed to have significant mobility at the instant of fracture, al-

though the water-cooled specimen temperature remains within 2–3°C of room temperature.

### Trapped Physical Entanglements

A possible explanation for the maximum in fracture energy, occurring at a certain  $M_C$  or crosslinker level is the contribution from physical entanglements. In any real network, physical entanglements are present in addition to the chemical crosslinks. At low crosslink levels, probably the physical entanglements dominate and at high crosslink levels, the chemical crosslinks dominate. This latter could be due to increased chain rigidity caused by the chemical crosslinks. Also, the number of trapped physical entanglements may be increasing with crosslinker, causing an increase in the fracture energy. Previously, it was remarked that the postulated increase in physical entanglements in homo-IPNs is controversial. The possible increase noted here in the number of physical entanglements with increasing chemical crosslink density is yet another point to be resolved. Beyond a certain crosslinker level, the increasing physical entanglements do not play a significant role in the fracture process, and the fracture energy is more dependent on the chemical crosslinks.

Langley<sup>28</sup> related the probability that a physical entanglement is trapped during the crosslinking process,  $T_e$ , to the gel fraction,  $W_g$ , of the network:

$$T_e = [2 - W_g - 2W_g \{\ln(1/1 - W_g)\}^{-1}]^2 \quad (9)$$

For a perfect network,  $T_e = 1$  and  $W_g = 1$ . How-



**Table VII Probability of Trapped Physical Entanglements in XPS and XPMMA**

mol % Crosslinker	Probability of Trapped Entanglements ( $T_e$ )		
	PS-AAA	PS-MAA	PMMA-AAA
0.5	$5.5 \times 10^{-4}$	$6.8 \times 10^{-3}$	0.09
1.0	$8.9 \times 10^{-3}$	NA	0.23
1.5	$8.9 \times 10^{-3}$	0.03	0.27
5.0	0.09	0.23	0.34
10.0	0.14	0.40	0.41

NA—not available.

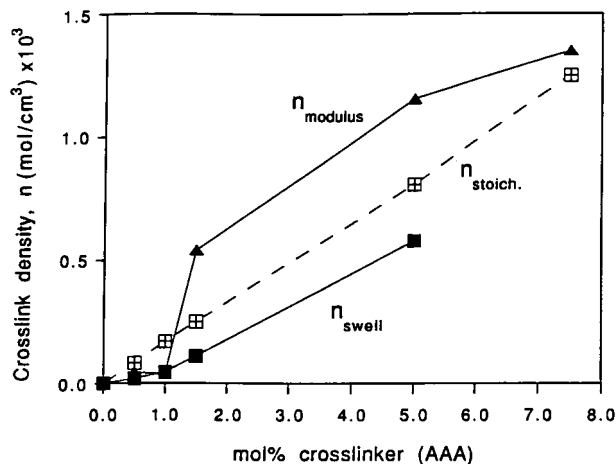
PS-AAA—acrylic acid anhydride crosslinked PS.

PS-MAA—methacrylic acid anhydride crosslinked PS.

PMMA-AAA—acrylic acid anhydride crosslinked PMMA.

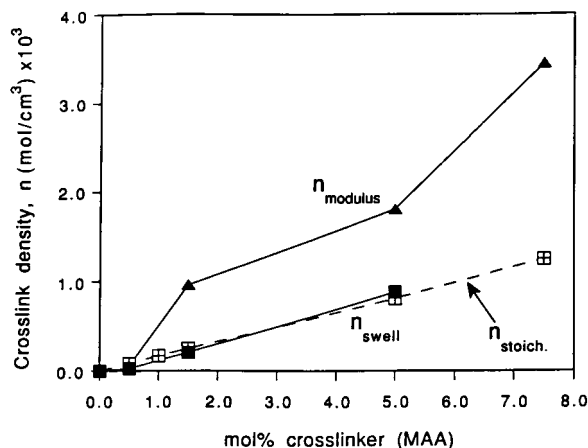
ever, this equation does not hold for low gel contents. From the gel fraction results given in Table I, the values for  $T_e$  were calculated using eq. (9). Results are shown in Table VII for the different networks. As given by eq. (9), the probability or the fraction of physical entanglements trapped in the networks, increases with crosslinker level. Physically, this means that crosslinking process brings the chains together, thereby increasing the number of entanglements. Values of  $T_e$  and  $W_g$  were used to calculate the total crosslink levels using the theories of Flory<sup>29</sup> and Scanlan.<sup>30</sup> The resulting values were lower than the experimental chemical crosslink level and showed no maximum, thus not adequately explaining the present findings.

In an attempt to verify the change in number of physical entanglements with crosslinking, the crosslink density from the plateau modulus measurements at 165°C [eq. (3)] were compared with that from the swelling measurements. Figures 3–5 compare the crosslink density values obtained from two different measurements as a function of the mol % crosslinker. The equilibrium swelling experiments are seen primarily measuring the chemical crosslinks, whereas the rubbery plateau modulus experiments provide a measure of the physical entanglements in addition to the chemical crosslinks. The difference between the two values can be considered as an estimate of the physical entanglement density. From Figures 3–5 it can be seen that the difference between the two changes with mol % crosslinker, with some suggestion of a maximum in Figures 3 and 5, but not in Figure 4. At very high crosslink levels, the


**Figure 3** Plot of crosslink densities from swelling and modulus measurements vs. mol % crosslinker for AAA crosslinked PS.

numbers calculated from the modulus measurements become independent of the crosslink level. However, rubber elasticity theory fails in this region, as does the Flory–Rehner equation. At higher crosslink levels (about 7.5 mol % crosslinker), the two crosslink densities seem to converge. Of course, the stoichiometric values increase linearly with mol % crosslinker (dashed lines in Figs. 3–5).

Miller and Kramer<sup>31</sup> studied the deformation of crosslinked PS films bonded to copper grids, strained in tension under a transmission electron microscope. Crosslinking of the films was carried out by electron beam irradiation in a controlled


**Figure 4** Plot of crosslink densities from swelling and modulus measurements vs. mol % crosslinker for MAA crosslinked PS.

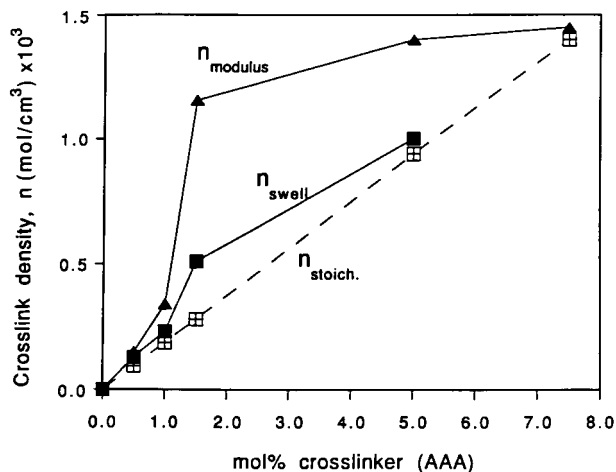


**Figure 5** Plot of crosslink densities from swelling and modulus measurements vs. mol % crosslinker for AAA crosslinked PMMA.

manner. They showed that failure mode in crosslinked polystyrene under tension changes from crazing to localized shear deformation with increasing crosslinking. This is analogous to the failure modes of PS and polycarbonate (PC) in tension.<sup>32</sup> Due to a lower entanglement density in PS ( $2 M_e \sim 32,000$  g/mol), it fails by crazing, whereas PC with a higher entanglement density ( $2 M_e \sim 2500$  g/mol) fails by shear deformation.

More importantly, Miller and Kramer<sup>31</sup> observed both crazing and shear deformation at a certain crosslinking level. When more than one micromechanism is operating in the system, more energy is consumed. This could possibly be true for the current systems at a certain crosslinker level, resulting in a maximum in the fracture energy. In this way, the molecular basis for fracture in plastics, including crosslinked plastics, is related back to micromechanical approach.

## CONCLUSIONS

Crosslinked PS and PMMA showed a maximum in the fracture energy at 1.5–5.0 mol % crosslinker level. For MAA crosslinked PS, the fracture energy remains higher than the uncrosslinked linear polymer at high crosslink densities, whereas in AAA crosslinked PS and PMMA, the fracture energy drops to near the initial value, uncrosslinked level. Using reversible crosslinkers, the number of chain scissions have been quantified. The number of chain scissions in-

creases asymptotically with crosslink density. The number of bonds activated per scission in the networks, obtained via indirect calculations of the chain scission energies is roughly a constant and is equal to the distance between physical entanglements in the uncrosslinked linear polymer, independent of the chemical crosslink density, up to about 1.5–5.0 mol % crosslinker. Beyond 5.0 mol % crosslinker, the decrease in fracture energy of XPS and XPMMA is attributed to chain immobility from chemical crosslinks. Rubbery plateau modulus measurements indicate that the physical entanglements trapped in the networks may be increasing with crosslinker. In essence, physical entanglements play a significant role in the fracture behavior of chemically crosslinked networks.

The companies that make up the Polymer Interfaces Center at Lehigh University are greatly appreciated. In addition, financial support through National Science Foundation Grant No. MSS-9212805 for the purchase of the Rheometrics RDA2 is greatly appreciated.

## REFERENCES

1. N. Mohammadi, A. Klein, and L. H. Sperling, *Macromolecules*, **26**, 1019 (1993).
2. M. Sambasivam, A. Klein, and L. H. Sperling, *Macromolecules*, **28**, 152 (1995).
3. A. J. Kinloch and R. J. Young, *Fracture Behavior of Polymers*, 2nd ed., Applied Science Publishers, London, 1983.
4. H.-H. Kausch, *Polymer Fracture*, 2nd ed., Springer Verlag, Berlin, 1987.
5. N. R. Langley and K. E. Polmanter, *J. Polym. Sci., Polym. Phys. Ed.*, **12**, 1023 (1974).
6. L. J. Broutman and F. J. McGarry, *J. Appl. Polym. Sci.*, **9**, 609 (1965).
7. J. P. Berry, *Fracture VII*, Liebowitz, Ed., Academic Press, New York, 1972.
8. P. J. Flory, N. Rabjohn, and M. C. Shaffer, *J. Polym. Sci.*, **4**, 435 (1949).
9. R. Natarajan and P. E. Reed, *J. Polym. Sci. A-2*, **10**, 585 (1972).
10. A. N. Gent, G. L. Liu, and M. Mazurek, *J. Polym. Sci., Polym. Phys. Ed.*, **32**, 271 (1994).
11. D. L. Siegfried, J. A. Manson, and L. H. Sperling, *J. Polym. Sci., Polym. Phys.*, **16**, 583 (1978).
12. J. R. Millar, *J. Chem. Soc.*, 1311 (1960).
13. K. Shibyama and Y. Suzuki, *Kobunshi Kagaku*, **23**, 24 (1966).
14. J. L. Thiele and R. E. Cohen, *Polym. Eng. Sci.*, **19**, 284 (1979).

15. M. Sambasivam, A. Klein, and L. H. Sperling, *J. Appl. Polym. Sci.*, **58**, 357 (1995).
16. M. Sambasivam, A. Klein, and L. H. Sperling, *Polym. Adv. Technol.*, **7**, 507 (1996).
17. L. H. Sperling, K. B. Ferguson, J. A. Manson, E. M. Corwin, and D. L. Siegfried, *Macromolecules*, **9**, 743 (1976).
18. P. J. Flory and J. Rehner, *J. Chem. Phys.*, **11**, 521 (1943).
19. L. H. Sperling, *Introduction to Physical Polymer Science*, 2nd ed., John Wiley & Sons, Inc., New York, 1992, p. 414.
20. K. E. Evans, *J. Polym. Sci., Polym. Phys. Ed.*, **25**, 353 (1987).
21. G. J. Lake and A. G. Thomas, *Proc. R. Soc. Lond. Ser. A*, **A300**, 108 (1967).
22. M. J. Sundell, E. O. Pajunen, O. E. Hormi, and J. H. Nasman, *J. Polym. Sci., Polym. Chem. Ed.*, **31**, 2305 (1993).
23. R. A. Pearson and A. F. Yee, *J. Mater. Sci.*, **24**, 2571 (1986).
24. (a) R. P. Wool, *Structure and Strength of Polymer Interfaces*, Hanser Press, New York, 1995; (b) R. P. Wool, *Macromolecules*, **26**, 1574 (1993).
25. H. Mark, *Cellulose and Cellulose Derivatives*, Vol. IV, Emil Ott, Ed., Interscience Publishers Inc., New York, 1943.
26. M. Sambasivam, A. Klein, and L. H. Sperling, *J. Polym. Mater.*, **13**, 1 (1996).
27. M. Sambasivam, A. Klein, and L. H. Sperling, in *Film Formation in Waterborne Coatings*, T. Proveder, M. A. Winnik, and M. W. Urban, Eds., ACS Symp. Ser. No. 648, American Chemical Society, Washington, DC, 1996.
28. N. R. Langley, *Macromolecules*, **1**, 348 (1968).
29. P. J. Flory, *Chem. Rev.*, **35**, 51 (1944).
30. J. Scanlan, *J. Polym. Sci.*, **43**, 501 (1960).
31. P. Miller and E. J. Kramer, *J. Mater. Sci.*, **25**, 1751 (1990).
32. E. J. Kramer, in *Advances in Polymer Science*, vols. 52/53, Springer Verlag, Berlin, 1983.